[Supplementary material]

Seaweed-eating sheep and the adaptation of husbandry in Neolithic Orkney: new insights from Skara Brae

Marie Balasse[1,*], Anne Tresset[1], Gaël Obein[2], Denis Fiorillo[1] & Henri Gandois[3]

[1] *UMR 7209 'Archéozoologie, archéobotanique: sociétés, pratiques, environnements', CNRS/MNHN, 55 Rue Buffon, 75005 Paris, France*

[2] *EA 2367 Laboratoire commun de Métrologie LNE-CNAM, CNAM, 61 Rue du Landy, 93210 La Plaine Saint-Denis, France*

[3] *UMR 8215 'Trajectoires—De la sédentarisation à l'Etat', Maison de l'Archéologie et de l'Ethnologie, 21 allée de l'Université, 92023 Nanterre, France*

[*] *Author for correspondence (Email: marie.balasse@mnhn.fr)*

Table S1. Provenience and dates of the selected sheep (*Ovis*) and cattle (*Bos*) second (M2) and third molars (M3). Dates after Bayliss *et al*. (2017). Highest $\delta^{13}C$ values within the tooth, and phase shift between $\delta^{13}C$ and $\delta^{18}O$ sequences as determined from the modelling.

Specimen ID	Context	Phase	Date cal BC	$\delta^{13}C_{max}$ (‰)	Phase shift (°)
SKB Ovis 3 M2	157	Phase 0	~ 3400-3100	-12,5	347
SKB Ovis 3 M3	157			-12,5	334
SKB Ovis 4 M3	168			-12,1	nd
SKB Ovis 17 M3	157			-12,6	332
SKB Ovis 2 M3	213	Phase 1	~ 2900-2825	-10,8	nd
SKB Ovis 12 M3	213			-12,8	308
SKB Ovis 13 M2	213			-9,3	177
SKB Ovis 13 M3	213			-9,2	nd
SKB Ovis 14 M3	213			-12,1	nd
SKB Ovis 1 M3	102	Phase 2	~ 2750-2500	-11,9	nd
SKB Ovis 5 M3	102			-12,0	317
SKB Ovis 6 M3	102			-8,2	146
SKB Ovis 7 M3	102			-7,9	199
SKB Ovis 8 M3	102			-7,4	204
SKB Ovis 9 M3	102			-9,0	175
SKB Ovis 10 M3	102			-11,6	nd
SKB Ovis 11 M3	102			-9,3	173
SKB Ovis 15 M3	102			-9,3	204
SKB Ovis 16 M3	102			-9,9	228
SKB Bos 6 M3	168	Phase 0	~ 3400-3100	-11,6	nd
SKB Bos 3 M3	213	Phase 1	~ 2900-2825	-11,3	nd
SKB Bos 4 M3	213			-11,2	nd
SKB Bos 5 M3	162			-12,1	285
SKB Bos 7 M3	213			-11,9	294
SKB Bos 10 M3	162			-11,7	303
SKB Bos 1 M3	102	Phase 2	~ 2750-2500	-10,1	nd
SKB Bos 2 M3	102			-11,2	nd
SKB Bos 8 M3	102			-11,4	nd
SKB Bos 9 M3	102			-11,4	nd

Table S2. Provenience and diet of the sheep used as references for pure grass, pure seaweed and mixed seaweed/grass diet. Highest $\delta^{13}C$ value measured in the annual cycle; phase shift between the $\delta^{13}C$ and $\delta^{18}O$ sequences. References: 1) this study; 2) Balasse *et al*. (2009); 3) Balasse *et al.* (2005).

Specimen ID	Location	Time period	Diet	Ref.	$\delta^{13}C_{max}$ (‰)	Phase shift (°)
ROU01 M2	Rousay (Orkney)	Modern	Grass	2	-15.8	333
ROU04 M2	Rousay (Orkney)	Modern	Grass	2	-16.0	298
ROU09 M2	Rousay (Orkney)	Modern	Grass	2	-15.1	296
ROU17 M2	Rousay (Orkney)	Modern	Grass	2	-16.5	307
ROU16 M2	Rousay (Orkney)	Modern	Grass	2	-15.6	301
ROU6 M2	Rousay (Orkney)	Modern	Grass	2	-15.1	303
KMZc128 M3	Kemenez (Brittany)	Modern	Grass	1	-15.4	340
KMZc119 M3	Kemenez (Brittany)	Modern	Grass	1	-14.9	315
KMZc123 M3	Kemenez (Brittany)	Modern	Grass	1	-15.1	340
KMZ00004 M3	Kemenez (Brittany)	Modern	Grass	1	-16.4	321
KMZ00018 M3	Kemenez (Brittany)	Modern	Grass	1	-15.6	330
KMZ10033 M3	Kemenez (Brittany)	Modern	Grass	1	-15.6	331
KMZ10026 M3	Kemenez (Brittany)	Modern	Grass	1	-15.2	327
KMZ22bisOvis1 M3	Kemenez (Brittany)	Bronze Age	Grass	1	-12.9	323
NROvis1 M3	North Ronaldsay (Orkney)	Modern	Seaweed	3	-2.6	320
SWN02 M2	North Ronaldsay (Orkney)	Modern	Seaweed	2	-4.6	342
NROvis3 M3	North Ronaldsay (Orkney)	Modern	Seaweed/grass	3	-1.9	218
NROvis4 M3	North Ronaldsay (Orkney)	Modern	Seaweed/grass	3	-3.6	222
NROvis5 M3	North Ronaldsay (Orkney)	Modern	Seaweed/grass	3	-4.6	183
NBN01 M2	North Ronaldsay (Orkney)	Modern	Seaweed/grass	2	-6.4	179
TWN05M2	North Ronaldsay (Orkney)	Modern	Seaweed/grass	2	-5.3	225

Table S3. Results from the modelling of the phase shift between the $\delta^{13}C$ and $\delta^{18}O$ sequences in sheep teeth (Rousay = ROU, Kemenez = KMZ and North Ronaldsay = NR, NBN, SWN and TWN).

	$\delta^{18}O$ (‰)				$\delta^{13}C$ (‰)			
Specimen	*A* (‰)	*D* (mm)	φ (°)	*M* (‰)	*A* (‰)	*D* (mm)	φ (°)	*M* (‰)
ROU01 M2	1.89	29.26	241.77	-4.27	0.69	29.26	268.45	-16.58
ROU04 M2	2.04	32.26	284.04	-4.41	0.71	32.26	345.70	-16.78
ROU09 M2	1.76	33.69	250.20	-4.39	0.68	33.69	314.13	-16.15
ROU17 M2	1.75	35.88	253.90	-4.14	0.61	35.88	306.45	-16.90
ROU16 M2	1.75	36.39	241.76	-4.53	0.73	36.39	300.84	-16.12
ROU6 M2	1.57	38.35	277.89	-4.05	0.74	38.35	334.53	-16.04
KMZc128 M3inf	1.19	17.70	282.31	-3.15	0.50	17.70	302.24	-15.84
KMZc119 M3inf	1.90	26.46	361.13	-2.28	1.67	26.46	406.27	-16.35
KMZc123 M3inf	1.71	23.41	350.19	-2.26	1.37	23.41	369.78	-16.72
KMZ00004 M3inf	1.27	23.06	378.22	-3.52	1.18	23.06	417.24	-17.76
KMZ00018 M3inf	1.55	22.96	309.88	-3.20	1.58	22.96	340.11	-17.10
KMZ10033 M3inf	0.87	24.58	307.10	-3.73	0.87	24.58	336.08	-16.71
KMZ10026 M3inf	1.11	23.80	276.15	-3.26	0.95	23.80	309.06	-16.57
KMZ22bisOvis1 M3	1.37	19.95	226.15	-3.26	1.04	19.95	-96.42	-14.16
NROvis1 M3	0.53	20.32	187.38	-4.53	0.69	20.32	227.21	-3.83
NROvis3 M3	0.81	25.22	278.68	-3.67	2.60	25.22	60.56	-4.60
NROvis4 M3	1.14	26.77	246.91	-3.62	1.67	26.77	384.44	-5.60
NROvis5 M3	0.93	32.50	281.84	-3.80	1.49	32.50	459.16	-6.25
NBN01 M2	0.52	25.21	215.15	-3.23	2.98	25.21	396.06	-9.48
SWN02 M2	0.51	26.91	266.88	-3.33	0.90	26.91	285.32	-5.66
TWN05 M2	0.65	25.55	221.97	-3.69	1.41	25.55	356.21	-6.56

The **$\delta^{18}O$** and **$\delta^{13}C$** sequences have been processed using a sinusoidal model approach. Although the anticipated pattern is not strictly sinusoidal, it is assumed to be periodic with the same period for both signals, corresponding to a full year. Moreover, the signal resulting mainly from an opposition between winter and summer, only two inflections per period are expected, with a smooth transition between the high and low signal. In this context, a sinusoidal model is the most adapted. Nevertheless, this assumption can be wrong in the particular case of a very brief period of seaweed consumption during winter, which could create two additional inflections not be taken into account with this model. Data were fitted by the following model:

$$\begin{cases} \hat{\delta}^{18}\mathrm{O}(d) = \mathrm{A}_{\delta^{18}\mathrm{O}} \sin\left(\frac{2\pi}{D} d + \varphi_{\delta^{18}\mathrm{O}}\right) + M_{\delta^{18}\mathrm{O}} \\ \hat{\delta}^{13}\mathrm{C}(d) = \mathrm{A}_{\delta^{13}\mathrm{C}} \sin\left(\frac{2\pi}{D} d + \varphi_{\delta^{13}\mathrm{C}}\right) + M_{\delta^{13}\mathrm{C}} \end{cases} \quad [1]$$

Where:

d is the distance in mm.
D is period of the signal in mm
$\varphi_{\delta^{13}\mathrm{C}}$ and $\varphi_{\delta^{18}\mathrm{O}}$ are respectively the phase for $\delta^{18}O$ and $\delta^{13}C$ in degree (°)
$M_{\delta^{13}\mathrm{C}}$ and $M_{\delta^{18}\mathrm{O}}$ are respectively the signal averages for $\delta^{18}O$ and $\delta^{13}C$ in ‰
$A_{\delta^{13}\mathrm{C}}$ and $A_{\delta^{18}\mathrm{O}}$ are respectively the signals magnitude for $\delta^{18}O$ and $\delta^{13}C$ in ‰

$A_{\delta^{13}\mathrm{C}}$, $A_{\delta^{18}\mathrm{O}}$, $M_{\delta^{13}\mathrm{C}}$, $M_{\delta^{18}\mathrm{O}}$, $\varphi_{\delta^{13}\mathrm{C}}$, $\varphi_{\delta^{18}\mathrm{O}}$ and *D* are adjusted simultaneously using a least square method.
From the fitted parameters, the phase shift between $\hat{\delta}^{18}\mathrm{O}(d)$ and $\hat{\delta}^{13}\mathrm{C}(d)$ is computed as

$$\Delta\varphi = \varphi_{\delta^{18}\mathrm{O}} - \varphi_{\delta^{13}\mathrm{C}} \quad [2]$$

Table S4. Results from the modelling of the phase shift between the $\delta^{13}C$ and $\delta^{18}O$ sequences in sheep and cattle teeth from Skara Brae (SKB), Holm of Papa Westray (HPWN) and Knap of Howar (KH). Highest $\delta^{13}C$ value measured in the sequence and phase shift between the $\delta^{13}C$ and $\delta^{18}O$ sequences.

	$\delta^{18}O$ (‰)				$\delta^{13}C$ (‰)					
Specimen	***A*** **(‰)**	***D*** **(mm)**	***φ*****(°)**	***M*** **(‰)**	***A*** **(‰)**	***D*** **(mm)**	***φ*****(°)**	***M*** **(‰)**	**$\delta^{13}C_{max}$ (‰)**	**Phase shift (°)**
SKB Ovis3 M2	1.81	28.30	247.44	-5.27	0.61	28.30	260.92	-13.10	-12.5	347
SKB Ovis3 M3	1.70	20.63	196.91	-4.24	0.56	20.63	222.60	-13.02	-12.5	334
SKB Ovis 17 M3	1.99	25.34	232.43	-5.71	0.57	25.34	260.76	-13.14	-12.6	332
SKB Ovis 12 M3	1.85	21.26	157.96	-5.70	0.42	21.26	209.92	-13.23	-12.8	308
SKB Ovis 13 M2	0.84	19.14	215.34	-4.30	1.34	19.14	38.78	-10.82	-9.3	177
SKB Ovis 5 M3	1.31	17.84	89.13	-2.96	0.70	17.84	131.67	-12.71	-12.0	317
SKB Ovis 6 M3	1.00	24.35	203.58	-4.58	1.66	24.35	57.46	-9.72	-8.2	146
SKB Ovis 7 M3	0.59	22.18	113.84	-3.58	1.31	22.18	-85.03	-10.72	-7.9	199
SKB Ovis 8 M3	1.13	20.70	134.75	-2.73	1.94	20.70	-69.40	-9.85	-7.4	204
SKB Ovis 9 M3	1.13	24.89	169.09	-4.13	1.61	24.89	-5.80	-10.72	-9.0	175
SKB Ovis 11 M3	0.89	20.87	75.74	-4.27	1.11	20.87	-96.95	-10.96	-9.3	173
SKB Ovis 15 M3	0.73	26.43	263.78	-5.08	1.79	26.43	59.53	-11.22	-9.3	204
SKB Ovis 16 M3	0.97	18.99	155.91	-4.86	0.78	18.99	-72.10	-10.98	-9.9	228
SKB Bos5 M3	0.88	43.56	199.98	-5.47	0.44	43.56	-85.42	-12.55	-12.1	285
SKB Bos 7 M3	0.60	43.18	176.75	-5.64	0.64	43.18	-117.29	-12.59	-11.9	294
SKB Bos 10 M3	0.74	41.44	238.96	-5.76	0.37	41.44	-63.66	-12.23	-11.7	303
HPWN Ovis1 M3	0.85	24.21	177.48	-3.85	3.15	24.21	386.70	-9.73	-6.7	151
HPWN Ovis3 M3	1.15	22.38	301.61	-3.67	3.03	22.38	113.92	-9.13	-5.8	188
HPWN Ovis4 M3	0.90	29.98	350.44	-3.92	2.82	29.98	189.04	-8.91	-5.7	161
HPWN Ovis5 M2	0.71	35.78	309.94	-3.67	2.67	35.78	118.70	-9.79	-7.0	191
HPWN Ovis7 M3	0.85	22.61	218.50	-2.79	2.80	22.61	50.99	-6.48	-4.1	168
HPWN Ovis8 M3	1.26	25.29	340.01	-3.03	1.79	25.29	153.58	-9.19	-7.1	186
HPWN Ovis9 M3	0.76	16.40	199.81	-3.58	1.55	16.40	36.89	-9.61	-8.2	163
HPWN Ovis10 M3	0.82	24.40	251.40	-2.59	1.62	24.40	34.19	-7.87	-6.3	217
HPWN Ovis11 M3	1.06	19.92	224.05	-3.54	0.91	19.92	49.69	-9.44	-8.6	174
HPWN Ovis12 M3	0.61	18.03	228.80	-3.12	2.63	18.03	53.55	-8.18	-5.6	175
KH Ovis7 M3	0.99	25.44	249.94	-4.23	0.36	25.44	95.72	-10.76	-10.2	154
KH Ovis9 M3	1.81	20.01	14.02	-3.94	0.36	20.01	21.92	-12.72	-12.2	352

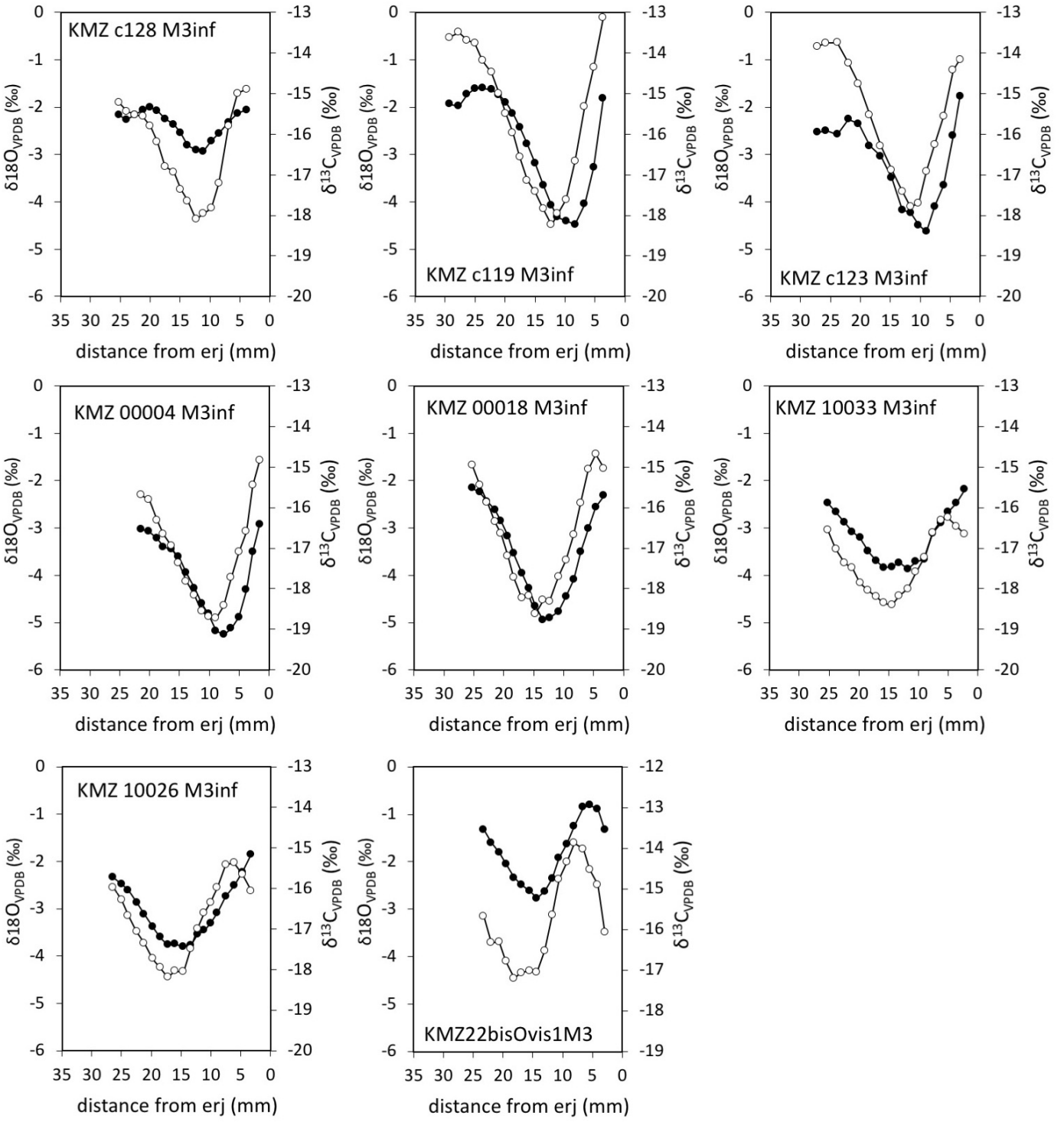

Figure S1. Results from sequential analysis of stable carbon ($\delta^{13}C$ in black) and oxygen isotope ratios ($\delta^{18}O$ in white) in the modern and Bronze Age ('22 bis') sheep from Kemenez.

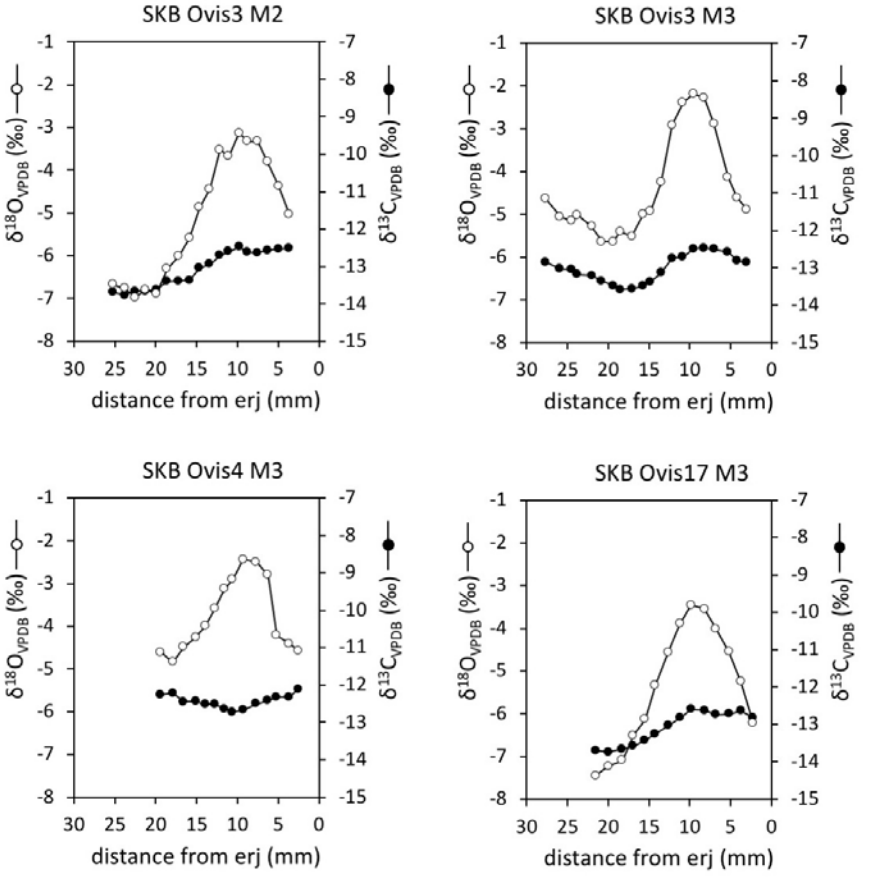

Figure S2. Results from sequential analysis of stable carbon ($\delta^{13}C$ in black) and oxygen isotope ratios ($\delta^{18}O$ in white) in sheep teeth from Skara Brae phase 0 (contexts 157 & 168).

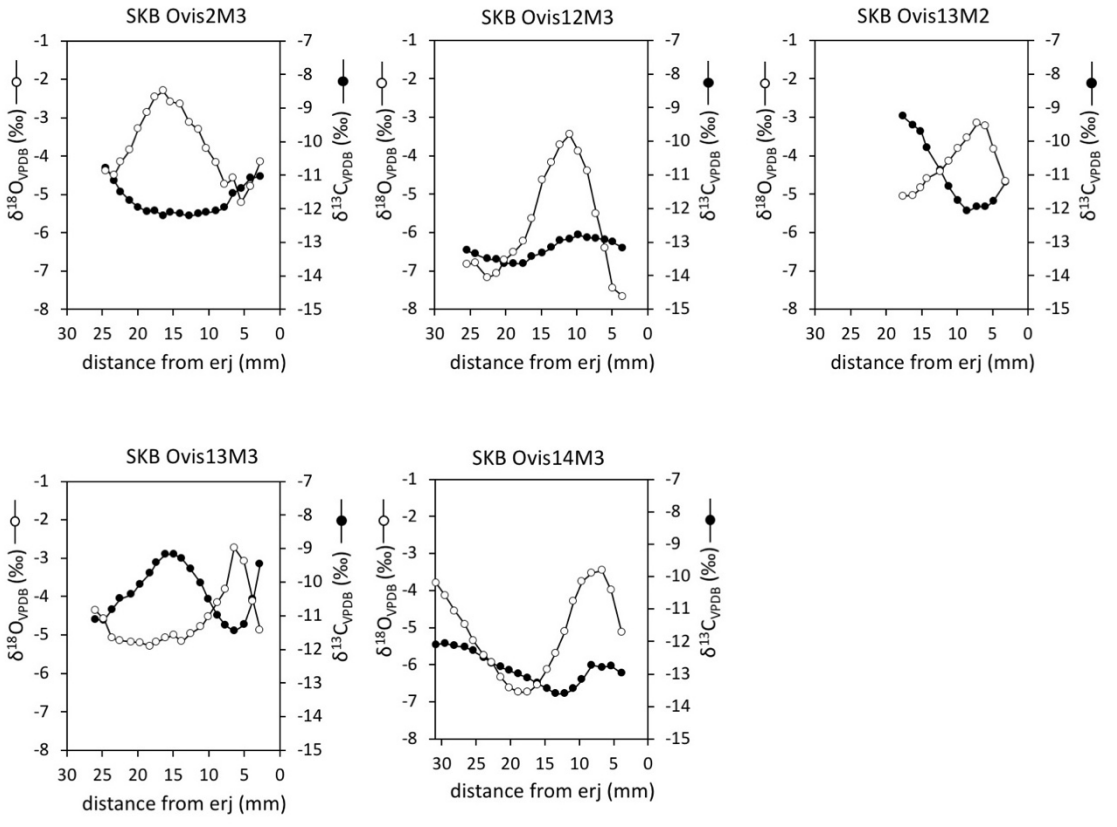

Figure S3. Results from sequential analysis of stable carbon ($\delta^{13}C$ in black) and oxygen isotope ratios ($\delta^{18}O$ in white) in sheep teeth from Skara Brae phase 1 (context 213).

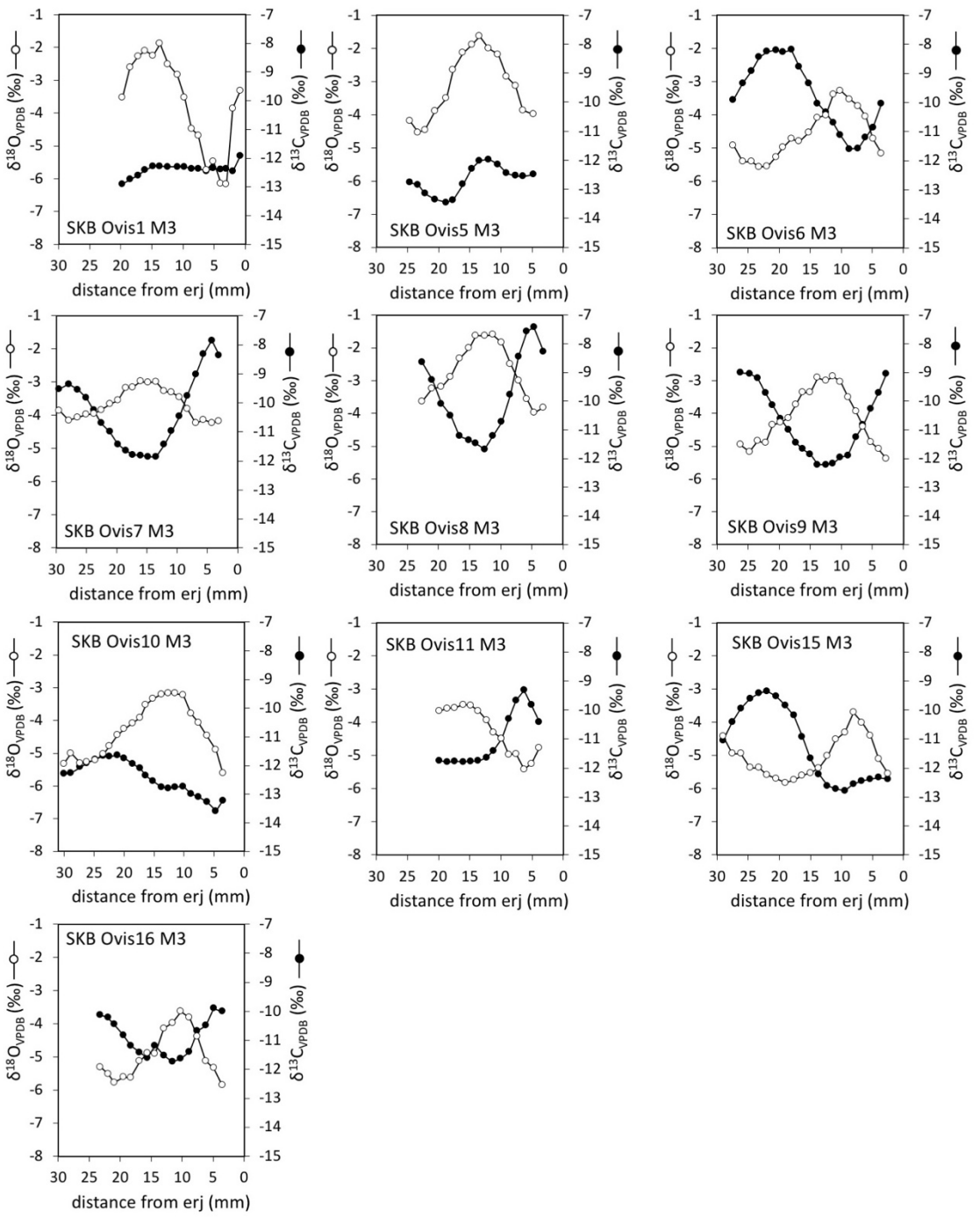

Figure S4. Results from sequential analysis of stable carbon ($\delta^{13}C$ in black) and oxygen isotope ratios ($\delta^{18}O$ in white) in sheep teeth from Skara Brae phase 2 (context 102).

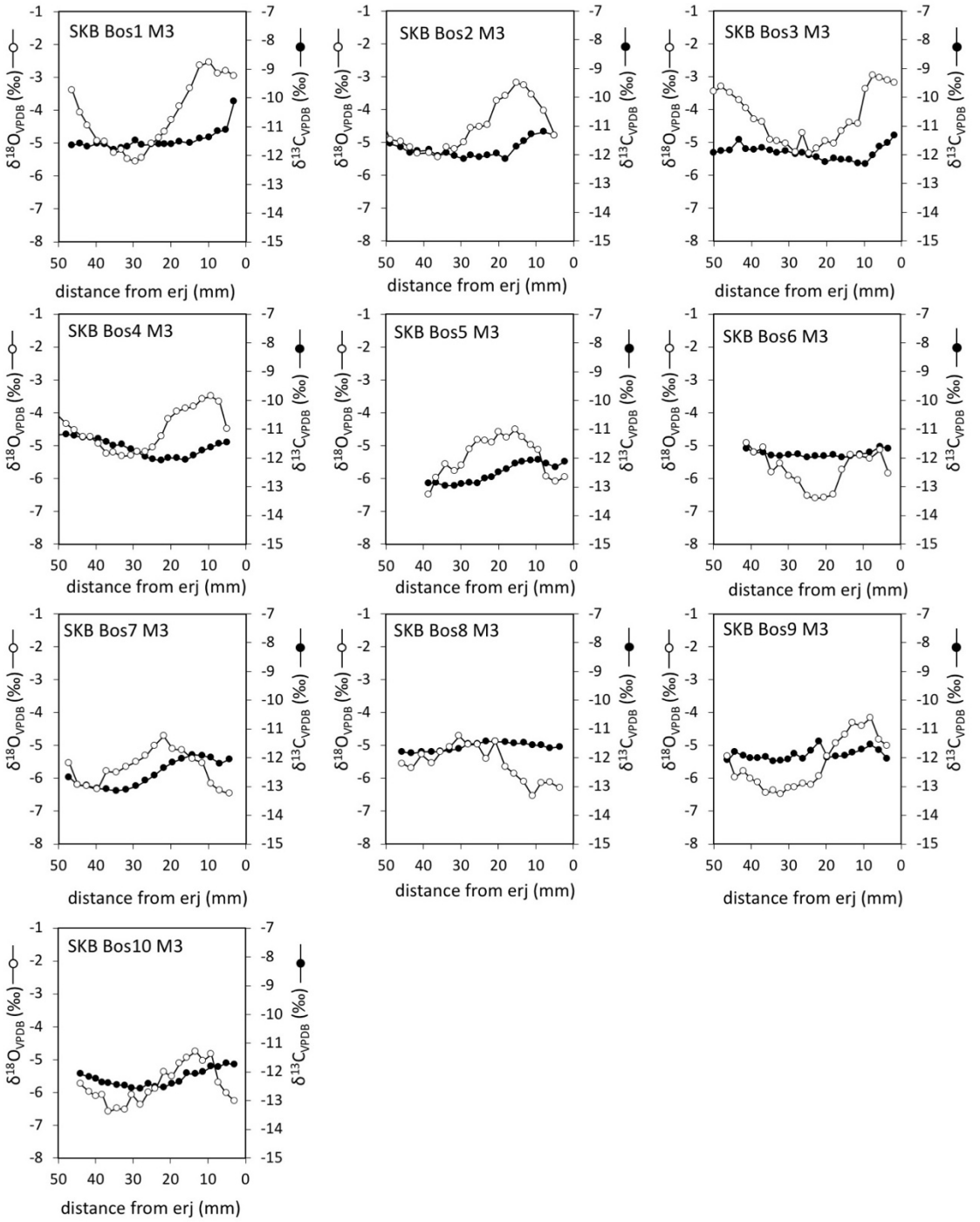

Figure S5. Results from sequential analysis of stable carbon ($\delta^{13}C$ in black) and oxygen isotope ratios ($\delta^{18}O$ in white) in cattle teeth from Skara Brae.

References

BAYLISS, A., P. MARSHALL, C. RICHARDS & A. WHITTLE. 2017. Islands of history: the Late Neolithic timescape of Orkney. *Antiquity* 91: 1171–88. https://doi.org/10.15184/aqy.2017.140

BALASSE, M., A. TRESSET, K. DOBNEY & S.H. AMBROSE. 2005. The use of isotope ratios to test for seaweed eating in sheep. *Journal of Zoology* 266: 283–91. https://doi.org/10.1017/S0952836905006916

BALASSE, M., I. MAINLAND & M.P. RICHARDS. 2009. Stable isotope evidence for seasonal consumption of seaweed by modern and archaeological sheep in the Orkney archipelago (Scotland). *Environmental Archaeology* 14: 1–14. https://doi.org/10.1179/174963109X400637